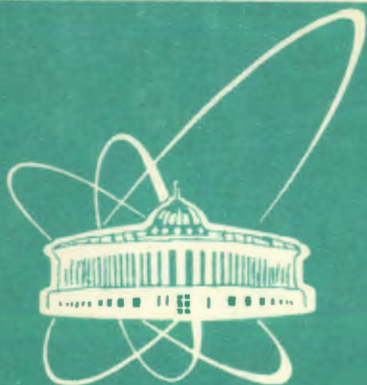


93-339



СООБЩЕНИЯ
ОБЪЕДИНЕННОГО
ИНСТИТУТА
ЯДЕРНЫХ
ИССЛЕДОВАНИЙ
ДУБНА

E13-93-339

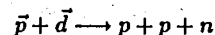
P.G.Akishin, V.I.Komarov, A.I.Puzynin

THE DETERMINATION
OF THE MAIN PARAMETERS
OF THE BACKWARD SPECTROMETER
OF THE «0° FACILITY»

1993

Introduction

In the paper [1] the exclusive deuteron break-up study with a polarized proton beam and a polarized deuterium gas target



at *COSY* - COoler SYnchrotron (Juelich, Germany) - was proposed. The main aim of the study is investigation of the cumulative process in its simplest, "elementary" form. The cumulative process can be picked out from others, background, processes in the most clear way if one of the final-state protons is detected at angles close to 180° with the large momenta near the kinematic limit. Detailed study of the process should be made in the exclusive way, which means that the momentum of the second proton must be also measured. The largest cross section of the process can then be obtained if this proton is detected at angles close to zero. In that way a collinear geometry of the process investigation becomes preferable. A special magnetic system called "0° Facility" [2] is very well suited for this purpose. The system consists of three dipole magnets installed on the internal beam of the ring accelerator (see Fig.1). They form a bump on the closed orbit of the proton beam. The first and the third magnets deflect the beam from its original position and turn it back. The central magnet serves as a spectrometric one for particles emitted at 0° angle and around of it from the target placed between the first and the second magnets. It is clear that, in principle, the first magnet can be used as a spectrometric magnet for the 180° emitted particles. However its original purpose consists in deflecting the primary beam and so the question arises whether this magnet can be effectively used as a spectrometric one for studying the cumulative break-up of the deuteron. The goal of the calculations described in this paper is to answer this question. So a simulation of the experiment aimed to optimize the detector geometry of the backward spectrometer and to estimate performance (angular and momentum acceptance and resolution) of the spectrometer. At the present time simulation of the experiment aimed to optimize the detector geometry and to estimate the spectrometer performance is being fulfilled.

The simulation program *COSY* serves these aims. We have interactive and batch program versions. The program was created on *IBM PC AT386*. As it is based on *GEANT3.14/16* system (see [3]), the program structure is analogous to other simulation programs which use this system (see for example [4]).

In this work the results of calculations aimed to define a position and dimensions, angular and momentum resolutions for the backward spectrometer of the "0° Facility" are presented.

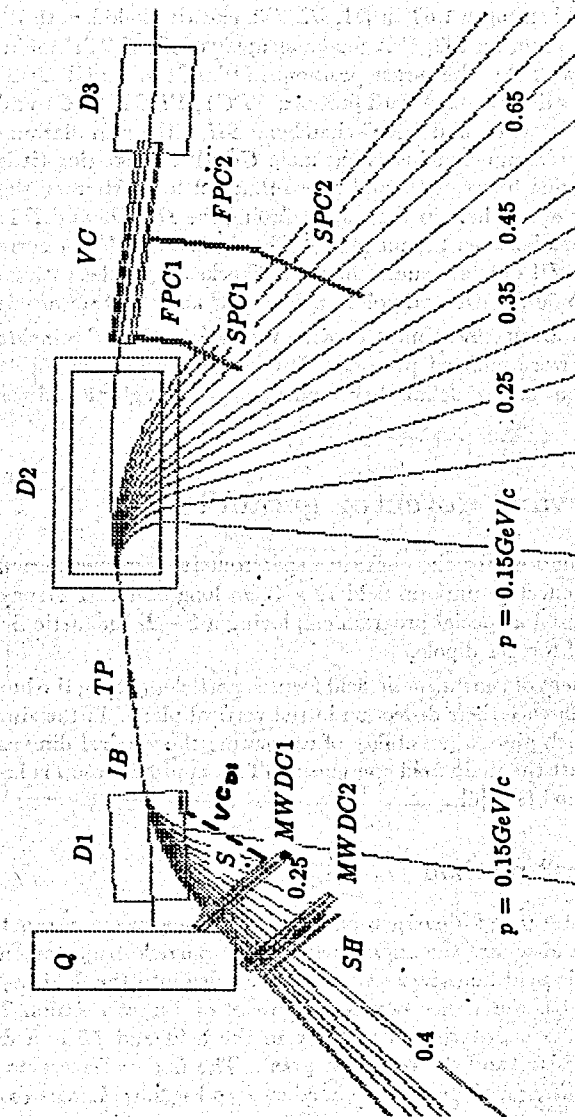
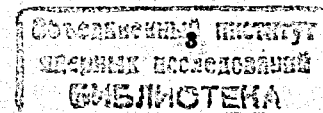


Fig.1. The detector arrangement for the deuteron experiment study (see text for details).



1. Experimental arrangement

In Fig.1 the detector arrangement of the "0° Facility" for the deuteron experiment is depicted. There *IB* denotes the internal *COSY* beam; *D1*, *D2*, *D3* are the dipole magnets (magnetic field strength 1.6T in *D1*, *D2*, *D3*; effective field length $79 \times 48\text{cm}$ for *D1*, *D3* and $158 \times 71\text{cm}$ for *D2*; *Q* is the quadrupole of the *COSY* main ring; *S* is the steel foil window; *TP* is the target position; *MWDC1* and *MWDC2* are the drift chambers for detecting the backward protons; *FPC1*, *FPC2*, *SPC1* and *SPC2* are the proportional "forward" and "side" chambers; *SH* is the scintillation counter hodoscope; *VC* is the vacuum chamber of the main *COSY* storage ring (it is shown in Fig.1 only in the region between *D2* and *D3* so that not to overburden the figure, but it comes certainly everywhere in the ring including the *D1*, *D2* and *D3* magnet gaps and direct sections between the magnets). The dashed line *VC*_{*D1*} corresponds to the boundary of the *D1* dipole vacuum chamber. Tracks of ejectiles with momenta from 150 MeV/c, step 50 MeV/c and polar angle $\theta = 0^\circ$ and $\theta = 180^\circ$ are depicted.

The experimental arrangement must provide the registration of coincidences of the backward and forward emitted protons. The backward detector [5] serves to detect backward protons and to define their momenta, polar angles θ and azimuthal angles φ .

2. The backward detector geometry

At the first step calculations for the backward spectrometer were performed in the approximation of the effective uniform field $79 \times 48\text{cm}$ long and 1.6T strong in the *D1* dipole. Later we used a special program employing a 2-D magnetic field map in the median plane of the *D1* dipole.

The main component of the magnetic field focuses particles only in the horizontal plane and does not influence their deflection in the vertical plane. In the simulation we used a method which gives a possibility of estimating the vertical dimensions of detectors if we have just the main field component. This approximation is known as the "thin lenses" method (see [6]).

2.1. "Thin lenses" method

Let us consider the entrance of a charged particle in a homogeneous magnetic field (see Fig.2). Here α_1 and α_2 are the angles between the particle trajectory and the normal to the magnetic field boundary (α_1 at the entrance into the field, α_2 at the exit from the field); *L1* is a distance between the point of Target Position *TP* and the field boundary, *L2* is a length of trajectory in the field and *L3* is a distance between the field boundary and the detection point. The Lorenz force acts on the particle moving in the fringing field near a boundary (see Fig.2.a). In this case (now

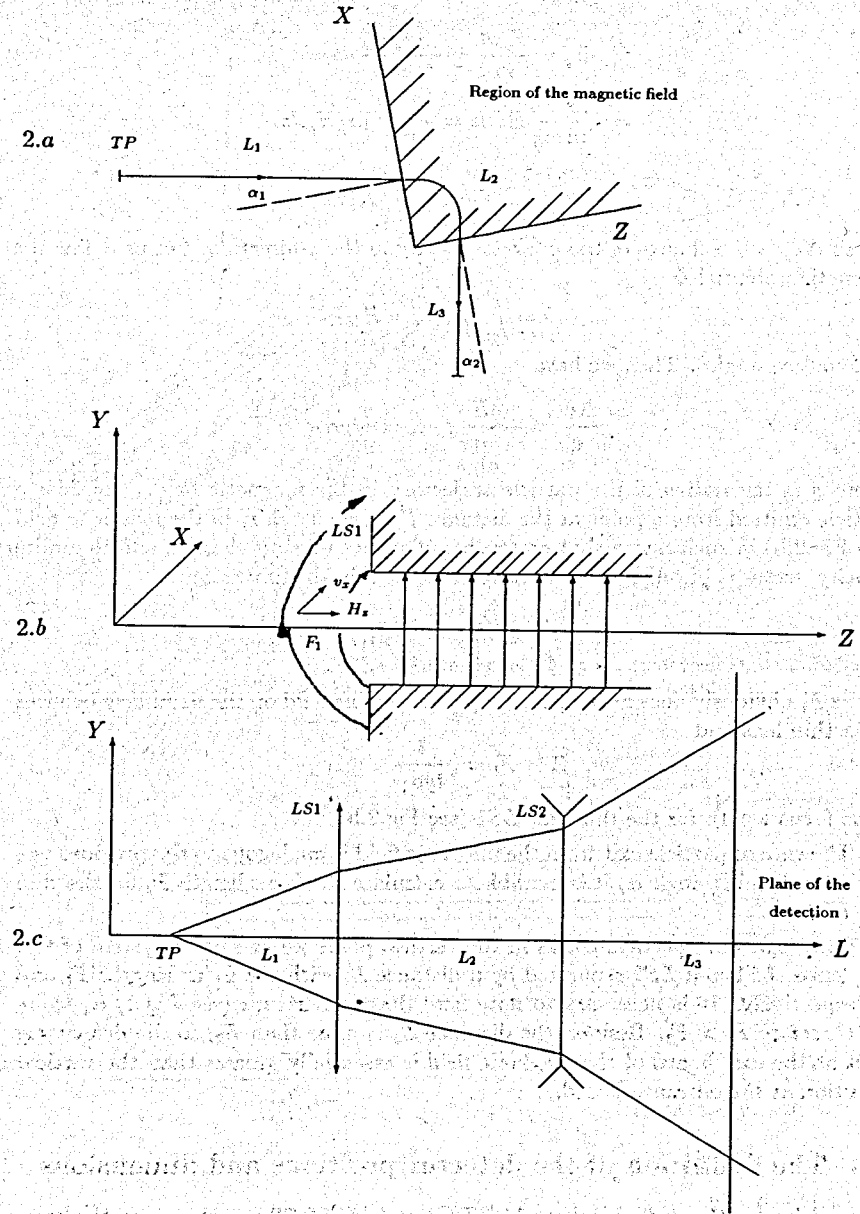


Fig.2. Geometry of the vertical focusing and defocusing on the boundaries.

we consider the entrance of the particle in the field):

$$dv_y = \frac{F_y dt}{m} = -\frac{ev_x H_z}{mc} dt =$$

$$= -\frac{e}{mc} \frac{v_x}{v_z} H_z dz = -\frac{e}{mc} tg\alpha_1 H_z dz,$$

or

$$\Delta v_y = -\frac{e}{mc} tg\alpha_1 \int_{out}^{in} H_z dz,$$

where Δv_y is the change of the particle velocity in the y -direction. Let us define the magnetic potential Φ as

$$\Phi = \int_{out}^{in} H_z dz = Hy$$

for small α_1 angles. Then we have

$$\frac{\Delta v_y}{v} = -\frac{eHy}{mvc} tg\alpha_1 = \frac{y}{\rho} tg\alpha_1,$$

where ρ is the radius of the particle trajectory in the magnetic field. Consider a particle emitted from a point at the distance F_1 to a boundary of the magnetic field (see Fig.2.b) in such a way that on the boundary its velocity changes and the finite velocity vector is parallel to the optical axis. Then in the first order

$$\frac{y}{F_1} = \frac{\Delta v_y}{v} = \frac{y}{\rho} tg\alpha_1,$$

and as F_1 obviously does not depend on y , the fringing field on the boundary behaves like a thin lens and

$$F_1 = \rho \frac{1}{tg\alpha_1}$$

is the focus length for the thin lens $LS1$ (see Fig.2.b).

The case of particle exit from the magnetic field is analogous to the previous one and after defining angle α_2 it is possible to calculate the focus length F_2 for the thin lens $LS2$.

So to calculate particle tracks in the vertical plane we can use a system of two thin lenses $LS1$ and $LS2$ separated by a distance L_2 with the focus lengths F_1 and F_2 respectively. It is necessary to note here that in our case (see Fig.3) $\alpha_1 < \alpha_2$ and therefore $F_1 > F_2$. Besides, the distance L_3 is more than L_2 , so the defocusing effect at the exit board of the magnetic field is essentially greater than the vertical deflection at the entrance board.

2.2. The definition of the detector positions and dimensions

The position for the drift chambers $MWDC1$ and $MWDC2$ was chosen on the basis of the following requirements:

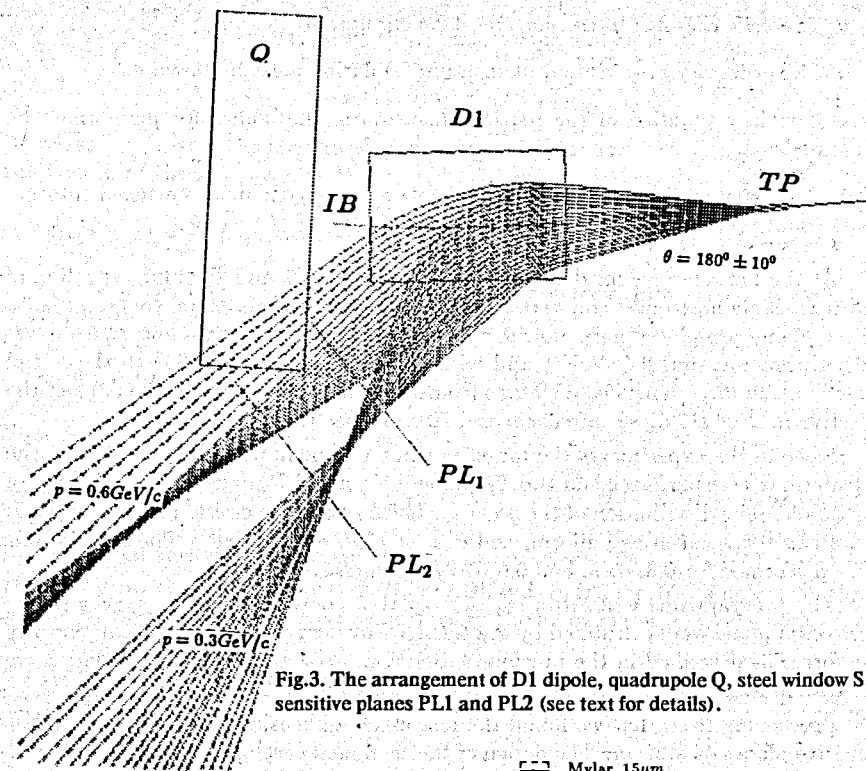


Fig.3. The arrangement of D1 dipole, quadrupole Q, steel window S, sensitive planes PL1 and PL2 (see text for details).

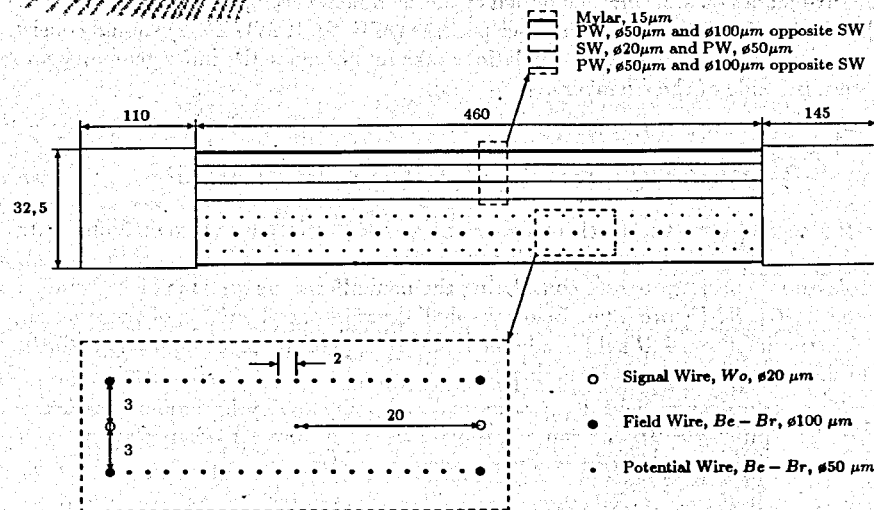


Fig.4. Geometry of the module in the multi-wire drift chamber.

- The drift chamber dimensions must be minimized.
- The necessary angular and momentum resolution must be provided.
- Certain separation of the particle momenta in the hodoscope plane must be realized.
- Geometry of the dipole and quadrupole arrangement must be taken into account.

At the first step we fixed two "sensitive planes" *PL1* and *PL2* for definition of the reasonable horizontal and vertical dimensions of the drift chambers (see Fig.3). These planes are placed perpendicular to the track of the protons emitted from *TP* with the momentum $0.45 \text{ GeV}/c$ and with the polar angle $\theta = 180^\circ$ to the initial *COSY* beam direction. The distances from *PL1* and *PL2* planes to the edge of the effective field of *D1* dipole are 35 cm and 70 cm respectively.

Since in the experiments the target position can be moved along the beam, the calculations were performed for two *TP* values: 40 cm and 75 cm from iron pole edge of *D1* dipole. The distribution of the polar angle θ for particles emitted from the target in all cases was taken as uniform, and $\theta_{\min} = 170^\circ$, $\theta_{\max} = 180^\circ$. The calculations were performed for 0.3 , 0.45 , and $0.6 \text{ GeV}/c$ momenta.

The program was written in such a way that coordinates of the tracks in the horizontal plane were calculated by the *GEANT* system and in the vertical plane by the formulas described in the previous subsection. As a result of the simulation we got distributions of the particle track intersections with *PL1* and *PL2* planes.

Proceeding from that we found the reasonable dimensions of the drift chamber sensitive planes $46 \times 22 \text{ cm}$. The design of the chambers developed by Dr. Zalikhanov [7] is depicted in Fig.4. Each chamber package (*MWDC1*, *MWDC2*) should consist of two such modules. All next simulations take into account the inner geometry and materials inside of the chambers.

3. Calculations with *D1* dipole field map

At the second step the track distributions in the vertical plane were found with more sophisticated calculations. We used a file with a $2-D$ field map for the *D1* dipole and a special program considering the nonuniform magnetic field and similar to the *ZGOUBI* [8] program. Below we shall describe the algorithm of the program reconstructing the $3-D$ field inside the magnetic gap of the dipole starting with the field distribution in the median plane.

Since a magnetic field \vec{B} in vacuum is a gradient of a harmonic function φ ($\vec{B} = \nabla\varphi$ and $\Delta\varphi = 0$), one can extrapolate the field from a median plane using a representation of space derivatives per plane derivatives.

In the median plane we have just a single component of field

$$B_z(x, y, 0) = \frac{d\varphi}{dz}(x, y, 0).$$

At a distance z from the median plane we can use the following Taylor expansion for calculation of the B_z -component

$$B_z(x, y, z) = \frac{d\varphi}{dz}(x, y, z) = \frac{d\varphi}{dz}(x, y, 0) + \frac{d^2\varphi}{dz^2}(x, y, 0)Z + \frac{d^3\varphi}{dz^3}(x, y, 0)\frac{Z^2}{2} + \dots$$

As $\Delta\varphi = 0$ and in the median plane $(x, y, 0)$ we have just the B_z -component ($B_x(x, y, 0) = B_y(x, y, 0) = 0$) then

$$\frac{d^2\varphi}{dz^2}(x, y, 0) = -\frac{d^2\varphi}{dx^2}(x, y, 0) - \frac{d^2\varphi}{dy^2}(x, y, 0) = -\frac{dB_x}{dx}(x, y, 0) - \frac{dB_y}{dy}(x, y, 0) = 0$$

Now

$$\frac{d^3\varphi}{dz^3}(x, y, 0) = -\frac{d^2}{dx^2} \frac{d\varphi}{dz}(x, y, 0) - \frac{d^2}{dy^2} \frac{d\varphi}{dz}(x, y, 0) = -\frac{d^2}{dx^2} B_z(x, y, 0) - \frac{d^2}{dy^2} B_z(x, y, 0)$$

and so on. In this way we present the space derivative $\frac{d\varphi}{dz}(x, y, z) = B_z(x, y, z)$ per derivatives on the median plane $\frac{d^2}{dx^2} B_z(x, y, 0)$ and $\frac{d^2}{dy^2} B_z(x, y, 0)$. The calculations for the B_z space component were performed in the following way. We have

$$B_z(x, y, z) = \frac{d\varphi}{dz}(x, y, z) = \frac{d\varphi}{dz}(x, y, 0) + \frac{d^2\varphi}{dx dz}(x, y, 0)Z + \frac{d^3\varphi}{dx dz^2}(x, y, 0)\frac{Z^2}{2} + \dots$$

In the median plane

$$\frac{d\varphi}{dx}(x, y, 0) = B_x(x, y, 0) = 0.$$

As $\Delta\varphi = 0$

$$\frac{d^3\varphi}{dx dz^2}(x, y, 0) = -\frac{d}{dx} \left(\frac{d^2\varphi}{dx^2}(x, y, 0) + \frac{d^2\varphi}{dy^2}(x, y, 0) \right) = 0.$$

Now

$$B_z(x, y, z) = \frac{d}{dx} B_z(x, y, 0)Z + \dots$$

and so on. All calculations for the B_y -component were performed in an analogous way as for the B_z -component.

At the median plane the program provides a fourth order interpolation with a 5×5 -points grid. In Fig.5 the behavior of B_z , B_y and B_x field components as a function of Z is depicted. As a distance between *D2* dipole iron poles is 9 cm we can see that in this "working region" our program gives a reliable picture of the field.

In Fig.6 we have depicted some characteristic results of this program for *GEANT* track tracing and "thin lenses" method calculations. We can see that these results (it is considered the vertical dimension Y) correspond to each other with a rather good accuracy.

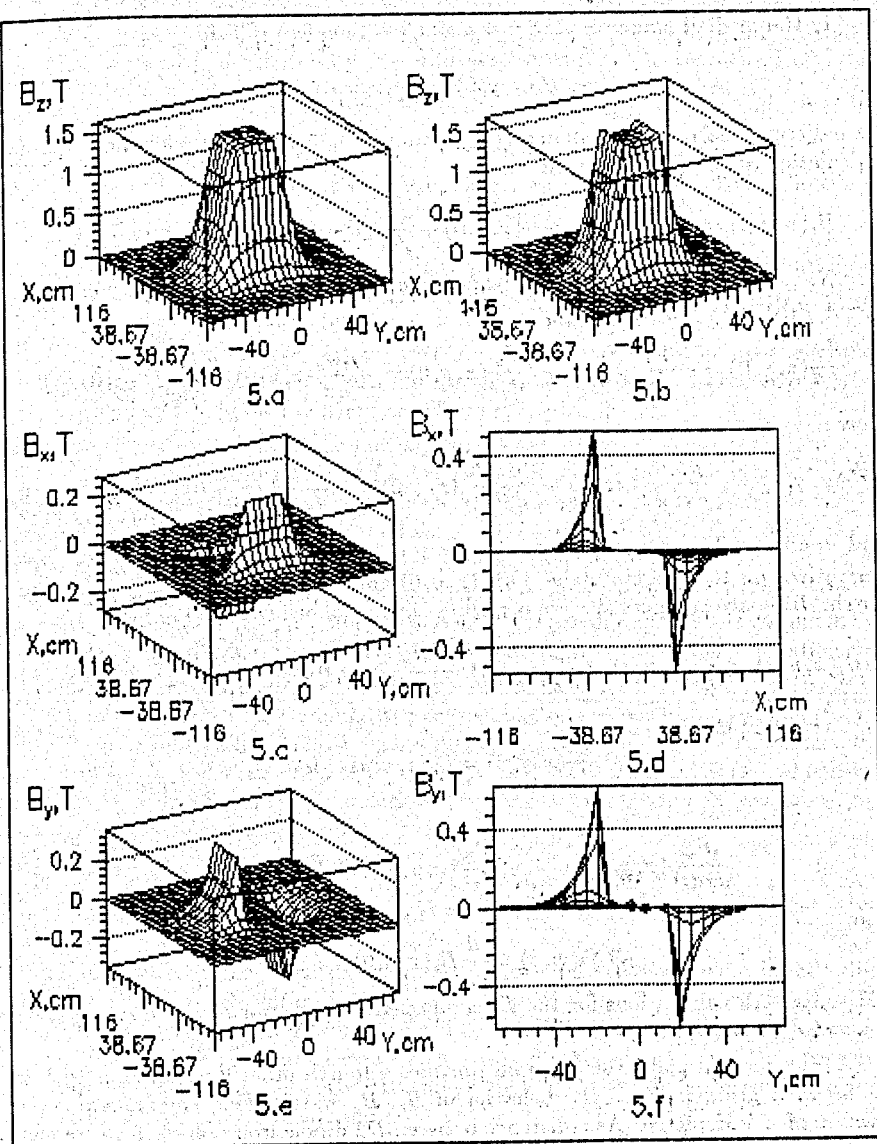


Fig.5. The behavior of the B_z , B_x and B_y components of the magnetic field for the dipole D1 as a function of Z (Z is a distance from the median plane):

- 5.a, 5.b: B_z if $Z=0$ cm -- in the median plane and $Z=4.0$ cm.
- 5.c, 5.d: B_x if $Z=2.5$ cm and $Z=4.0$ cm.
- 5.e, 5.f: B_y if $Z=2.5$ cm and $Z=4.0$ cm.

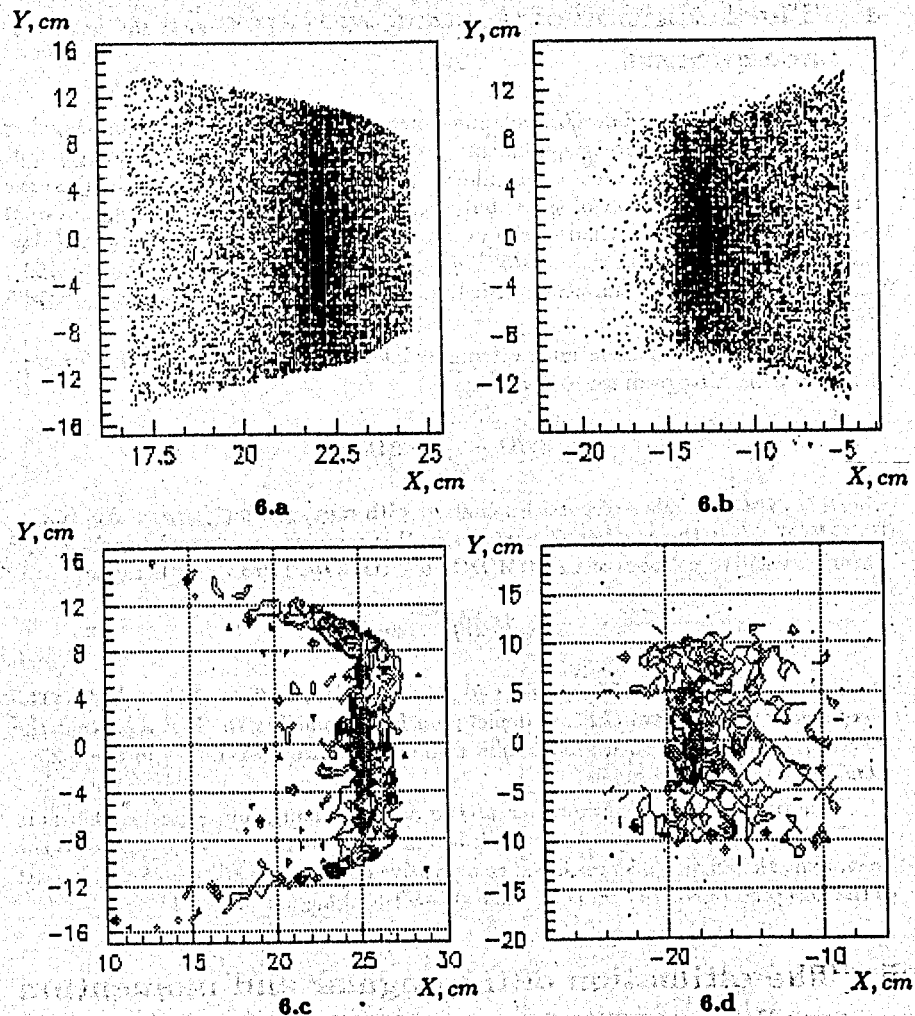


Fig.6. The distribution of particle track intersections with a central plane PL2 of the MWDC2 chamber (distributions (a,b) were got using "thin lenses" method).
 6.a.: TP=75cm, p=300 MeV/c; 6.b.: TP=75cm, p=600 MeV/c;
 6.c.: TP=75cm, p=300 MeV/c; 6.d.: TP=75cm, p=600 MeV/c.

4. The definition of the backward-proton detector acceptance

Here we take into consideration certain geometry of the $D1$ dipole vacuum chamber determined by the technical requirements. In Fig.1 the dashed line VC_{D1} corresponds to the boundary of the vacuum chamber. All particles crossing the VC_{D1} line are thrown away. The number of simulated events for each of the TP values was equal to $1.5 \cdot 10^5$. The distribution of the polar angle θ for emitted particles was taken uniform, for $TP = 40\text{cm}$ $\theta_{min} = 155^\circ$, $\theta_{max} = 180^\circ$, for $TP = 75\text{cm}$ $\theta_{min} = 164^\circ$, $\theta_{max} = 180^\circ$, the momentum p was varied uniformly from $p_{min} = 0.15$ to $p_{max} = 1.05$ GeV/c .

We divided the momentum spectrum at intervals $\Delta p = 10\text{MeV}/c$ and for each channel of the histogram we took a value

$$\Delta\Omega_i = \frac{N_i}{N_{0i}} \cdot \Delta\Omega_0,$$

where N_{0i} is the number of particles emitted with momenta $p \in [p_i; p_i + \Delta p]$ ($\Delta p = 10\text{MeV}/c$), N_i is the number of particles in this momentum interval which passed through sensitive volumes of the $MWDC1$ and $MWDC2$ drift chambers and

$$\Delta\Omega_0 = 2\pi \int_{\theta_0}^{180} \sin\theta d\theta.$$

For $TP = 40\text{cm}$ $\theta_0 = 155 \cdot \pi/180$ and for $TP = 75\text{cm}$ $\theta_0 = 164 \cdot \pi/180$. The acceptances for these two TP are depicted in Fig.7a and Fig.7b. It is seen that the spectrometer provides rather high solid angle acceptance ($\sim 0.1\text{ster}$) in the $0.25 - 0.60\text{GeV}/c$ momentum range.

Acceptance of the spectrometer at the angular-momentum plane is shown in Fig.7 c,d. (If the emitted particle track lies in the right hemisphere relative to the beam axis, the angle θ is determined as a positive one.) It is seen that the main part of the accepted particles occurs at the $\theta \in [-5^\circ; +5^\circ]$ angular interval.

5. The estimation of the angular and momentum resolution

The deuteron break-up study [1] experiment is one of the experiments at the internal $COSY$ beam. Determination of momenta and polar angles in such experiments has some specific features. The main peculiarity is measuring of the track coordinates only after passage of the particle through the field of the spectrometric magnets. Since in this case the emission angle and momentum of the particle can be found only with the known emission point, it is important to find the influence of the finite dimensions of the target on the spectrometer resolution. For estimation of

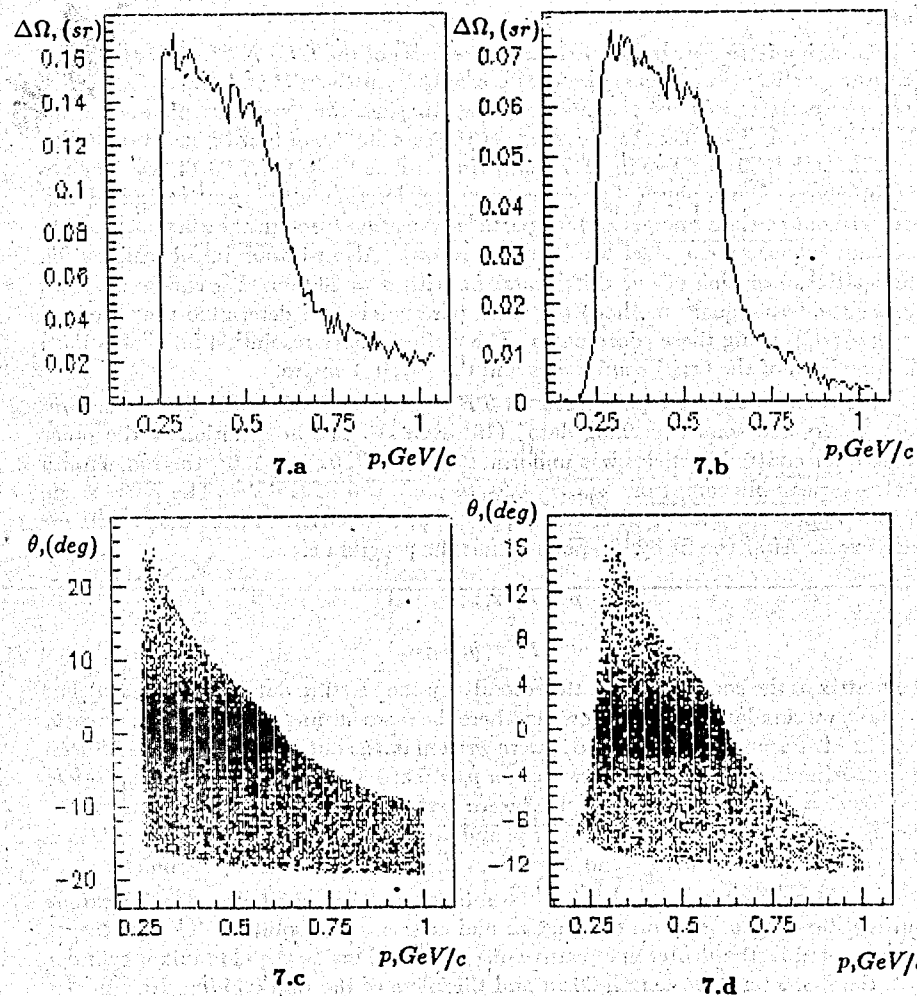


Fig.7. The acceptance of the backward-proton detector as a function of the particle momentum p (a,b) and the angular-momentum acceptance of the backward detector (c,d) (see text for details).

7.a,c: $TP = 40$ cm;

7.b,d: $TP = 75$ cm.

the angular and momentum resolution in this case the fitting program, written by Dr. O.E. Gorchakov [9] can be used. The input parameters for this program are coordinates $(x; y)$ of particle trajectory intersections with the first "sensitive plane" of the *MWDC1* and angles $(\alpha_x; \alpha_y)$ between tracks and *OX, OY* axis in the *MWDC1* plane.

Our simulation program (created on the basis of the *GEANT3.14* system) generates a particle (in our case, proton) escaping from the *TP* and traces it through the spectrometer. When the proton passes through the "sensitive planes" of the *MWDC1* and *MWDC2* chambers we get the coordinates of four intersection points (two in *MWDC1* and two in *MWDC2*). In our case the *GEANT3.14* system gives the influence of such physical processes as energy losses, multiple scattering and others (without nuclear interaction) for particle transition through the current tracking medium (mylar layers, steel windows and so on). Also we took into consideration the spatial resolution of our drift chambers with $\sigma = 200\mu m$. We can reconstruct (using the least-square method) the track parameters and determine the values of $(x; y; \alpha_x; \alpha_y)$, using these coordinates. The drift chamber resolution influences both the precision of the $(x; y)$ coordinates and the $(\alpha_x; \alpha_y)$ angles.

All calculations were performed for $TP = 40cm$ and $TP = 75cm$. At the first step we created some "teaching data" (10^4 events). The distribution of the polar angle θ for emitted particles was uniform, $\theta_{min} = 156^\circ$, $\theta_{max} = 180^\circ$, the momentum p also varies uniformly from $p_{min} = 0.24$ to $p_{max} = 0.75 GeV/c$. The polar angle θ , the momentum p and parameters $(x; y; \alpha_x; \alpha_y)$ were written in the output file for each event. After the fit by the polynomials the program creates

$$p = F_p(x; y; \alpha_x; \alpha_y)$$

$$\theta = F_\theta(x; y; \alpha_x; \alpha_y)$$

the matrix of the coefficients. At the second step the "testing data" were created. For example we simulated about 10^3 events where the momentum p_i and the polar angle θ_i were fixed. Parameters $(x; y; \alpha_x; \alpha_y)$ were written in the output file. The calculations in approximations of the "point target" for $p_i = 0.3; 0.35; 0.4; 0.45; 0.5; 0.55; 0.6 GeV/c$ and for $\theta_i = 180^\circ; 178^\circ; 176^\circ; 172^\circ; 168^\circ$ were performed. After the reconstruction we had distributions of events over p near p_i and over θ near θ_i . The standard deviations of these distributions were found, that gives the resolution of the spectrometer.

At the next step we estimated the influence of the gas target spatial extent and real target geometry on the angular and momentum resolution. The gas target was accepted as the deuteron extensive one contained inside the aluminium cylinder with the diameter $2cm$, length $20cm$ and thickness of the wall $0.5mm$. Now in our simulation program the vertices of the initial beam interactions with the gas target are distributed in the cylinder with diameter $2mm$ (the diameter of the initial beam) and length $20cm$. The distribution parameters data were taken from paper [10]. This "interaction region" is placed around the axis of the aluminium cylinder. In Fig.8-Fig.9 we plotted the momentum and angular resolutions as a function of the momentum.

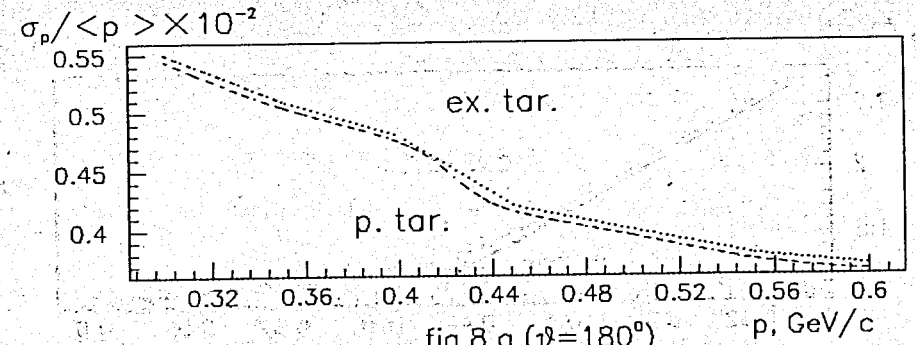


fig.8.a ($\vartheta=180^\circ$)

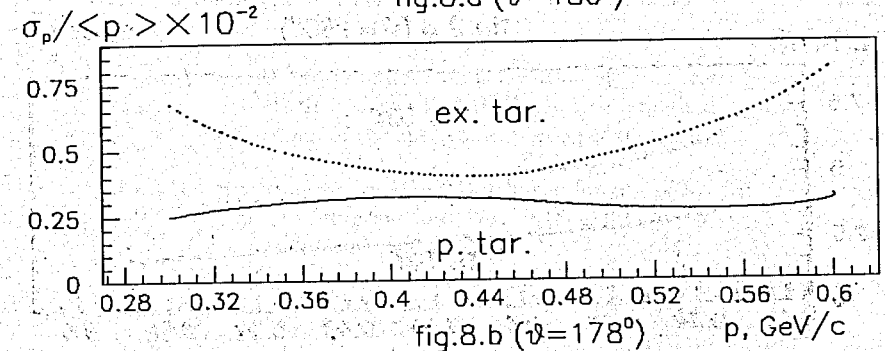


fig.8.b ($\vartheta=178^\circ$)

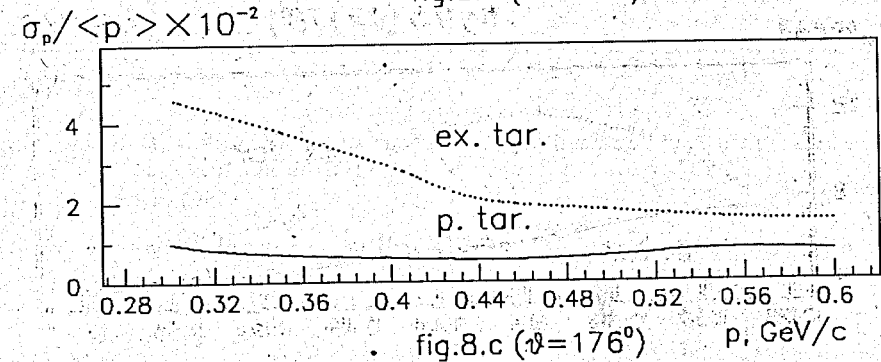


fig.8.c ($\vartheta=176^\circ$)

Fig.8. The momentum resolution as a function (using splines) of the particle momentum in approximation of the extensive gas target (ex. tar.) and point target (p. tar) for $TP = 40cm$.

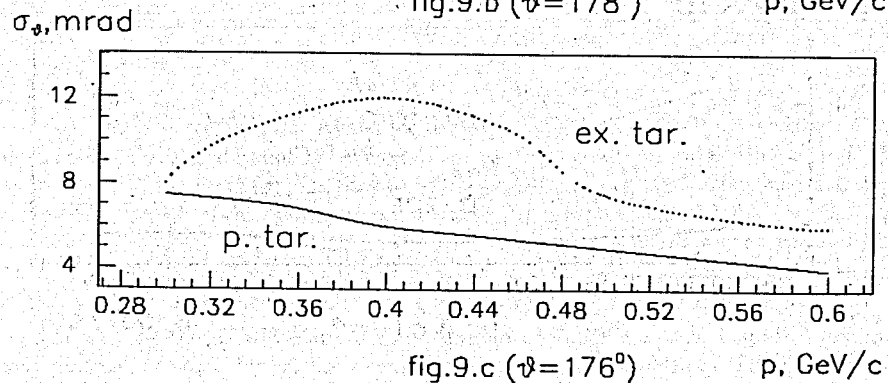
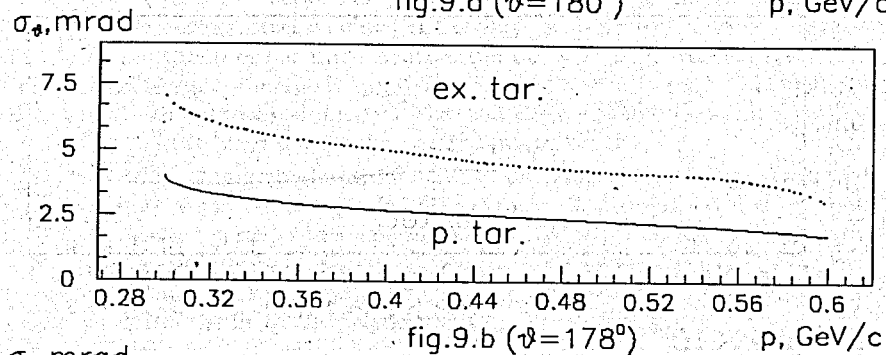
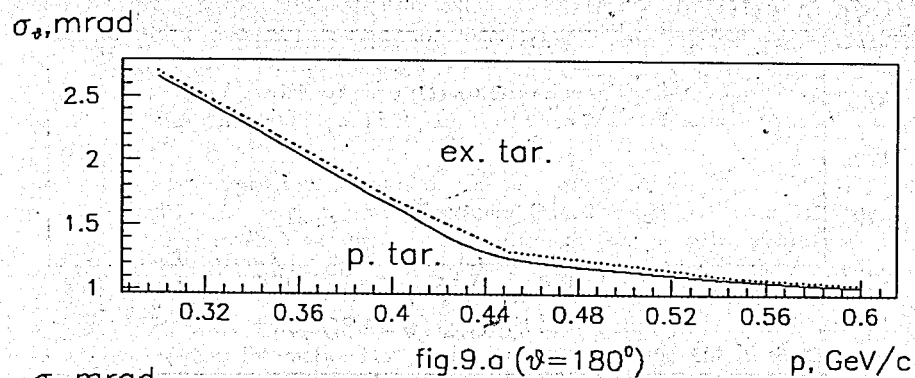


Fig.9. The angular resolution as a function (using splines) of the particle momentum in approximation of the extensive gas target (ex. tar.) and point target (p. tar.) for $TP = 40\text{cm}$.

6. Conclusion

In the conclusion we point out some results of the work:

- The main geometric parameters of the "0° Facility" backward detector have been determined.
- The expected performance of the backward spectrometer has been calculated for the chosen design of the detector chambers. It is sufficiently good for the purpose of the deuteron break-up study and investigation of a wide range of cumulative processes.
- The comparison of the two methods for calculation of track tracing in magnetic field has been realized. It is shown that the "thin lenses method" can be successfully used for estimation of the spectrometer acceptance.

We express our gratitude to Dr. O.E. Gorchakov for use of his fitting program and Dr. V.V. Ivanov for fruitful discussion. We are thankful also to Dr. M. Buesher for assignment of the magnetic field maps.

This work was supported by the Russian Foundation for the Fundamental Research (93-02-3745).

References

- [1] W. Borgs et. al. *Proposal for Exclusive Deuteron Break-up Study with Polarized Protons and Deuterons at COSY*
IKP, Juelich, 1992.
- [2] V. Abaev et. al. *Proceedings of the Workshop "Meson Production, Interaction and Decay"*
Cracow, 1991. World Scient. Publ. Co., Singapore, 1991, p.259.
- [3] R. Brun et al.: *GEANT3 Program Library* CERN, Data Handling Division DD/EE/84-1, 1987.
- [4] P.V. Zrelov et. al. *Simulation of the Experiment for Investigation of Subthreshold K^+ -Production*
MATEMATICHESKOE MODELIROVANIE, (in russian), v4/11/1992, p.56-74.
- [5] V.I. Komarov et. al. *Development of the Backward Detector System for the "0° Facility"*
IKP Annual Report 1992, KFA Juelich, p.26.

- [6] D. Lukkey in *Techniques of High Energy Physics*. Edited by David M. Ritson. Interscience Publishers, INC, New York
Interscience Publishers, LTD, London 1961
- [7] L.V. Horn et. al. *Testing of a Module of the Multiwire Drift Chamber for the "0° Facility"*
IKP Annual Report 1992, KFA Juelich, p.30.
- [8] F. Meot and S. Valero. *ZGOUBI Users Guide*.
Laboratory National Saturne, 1990.
- [9] Gorchakov O.E. *Advantages of Gramm-Schmidt Orthogonalization Method as Compared with the Forsythe Method at Multidimensional Approximation*
P11-84-188, JINR, Dubna, 1984.
- [10] Mishnev S.I. et. al. *Polarized Deuterium Target in an Electron Storage Ring: Measurement and Perspectives*.
Institute of Nuclear Physics, Novosibirsk, 1988.

Received by Publishing Department
on September 17, 1993.